

## Single crystal growth and structure of $\text{La}_4\text{Cu}_3\text{MoO}_{12}$

James A. Enterkin<sup>b</sup>, Paul A. Maggard<sup>b,1</sup>, Shintaro Ishiwata<sup>a</sup>, Laurence D. Marks<sup>c</sup>,  
Kenneth R. Poeppelmeier<sup>b,\*</sup>, Masaki Azuma<sup>a</sup>, Mikio Takano<sup>a</sup>

<sup>a</sup> Institute for Chemical Research, Kyoto University, Uji, Kyoto-fu 611-0011, Japan

<sup>b</sup> Department of Chemistry, Northwestern University, 2145 Sheridan Road, Evanston, IL 60208-3113, USA

<sup>c</sup> Department of Materials Science and Engineering, Northwestern University, 2220 North Campus Drive, Evanston, IL 60208-3108, USA

### ARTICLE INFO

#### Article history:

Received 17 July 2009

Received in revised form

17 October 2009

Accepted 21 November 2009

Available online 23 December 2009

#### Keywords:

$\text{La}_4\text{Cu}_3\text{MoO}_{12}$

Single crystal growth

Flux growth

Hexagonal  $\text{YAlO}_3$

### ABSTRACT

We report the synthesis and structure determination of single crystals of  $\text{La}_4\text{Cu}_3\text{MoO}_{12}$  grown from a  $\text{CuO}/\text{KCl}$  flux. This material, whose structure had previously been reported based solely on polycrystalline diffraction data, shows frustrated magnetic behavior and an anti-ferromagnetic ordering of spin-1/2 triangles at low temperatures. The structural and atomic parameters determined from the single crystal data are in very good agreement with those reported previously. However, HREM data showed evidence for disorder in the stacking of the  $\text{Cu}_3\text{MoO}_4$  planes, and thus a twinned structural refinement in space group  $P2_1/m$  was replaced by an equivalent disordered structural model in space group  $Pm$ . This development of a synthetic route to single crystals of  $\text{La}_4\text{Cu}_3\text{MoO}_{12}$  will allow a more detailed investigation of its complex electronic and magnetic properties.

© 2009 Elsevier Inc. All rights reserved.

### 1. Introduction

Transition metals with unpaired  $d$ -electrons, such as  $\text{Cu}^{2+}$  ( $d^9$ ;  $S=1/2$ ), can display a variety of magnetic behaviors beyond the familiar ferromagnetic or anti-ferromagnetic properties. Systems in which competing magnetic interactions make a single ordered ground state impossible are known as “frustrated”. Investigations of frustrated spin systems are of interest not only for their unusual magnetic behavior, but also because of their far-reaching implications with respect to spin glasses and even how water freezes into ice [1].

A simple example of a frustrated system is a two-dimensional triangular lattice of antiferromagnetically interacting spins. When magnetic spins are placed on the vertices of the triangles it becomes impossible to satisfy all of the anti-ferromagnetic interactions—only two of the three spins can be aligned anti-parallel simultaneously. The layered lattice of  $\text{La}_4\text{Cu}_3\text{MoO}_{12}$  resembles such a frustrated system with slightly distorted  $\text{Cu}_3\text{O}$  triangular clusters isolated by  $\text{MoO}_5$  trigonal bipyramids, shown in Fig. 1. The overall structure is derived from the hexagonal  $\text{YAlO}_3$  structure type with a 3:1 ordering of  $\text{Cu}^{2+}$  and  $\text{Mo}^{6+}$  cations superimposed on the metal site. This structure was recently determined based on combined powder X-ray, electron and neutron diffraction data by Vander Griend et al. [2].

Magnetic susceptibility, high-field magnetization and specific heat measurements on polycrystalline samples of  $\text{La}_4\text{Cu}_3\text{MoO}_{12}$  have shown that its magnetism is best described by three distinct temperature regimes [2,3]. At high temperatures, individual  $\text{Cu}^{2+}$  spins act independently to produce a paramagnetic state. Below 250 K, strong intra-triangle anti-ferromagnetic interactions align two of the three spins to yield trimers with  $S_{\text{total}}=1/2$ . The localized moments on the trimers, which now form a square net, then align antiferromagnetically below 2.6 K as a result of weak inter-trimer interaction. Inelastic and elastic magnetic neutron scattering experiments have gauged the intra-trimer coupling constants and revealed that the inter-trimer ordering doubles the unit cell along the  $a$  direction. Recent theoretical studies have attempted to determine how the intra-triangle coupling affects the long-range ordering wave vector of the low-temperature phase [4–6]. To relate theoretical predictions to the true magnetic ground state, single crystals are often necessary because anisotropic properties, such as the magnetization or electron spin resonance absorption, can then be measured along each unique axis. Unfortunately, single crystals of complex metal oxides are notoriously difficult to obtain. In this communication, we report the growth of  $\text{La}_4\text{Cu}_3\text{MoO}_{12}$  single crystals from a  $\text{CuO}/\text{KCl}$  flux. The development of a route to single crystal growth should pave the way for more detailed magnetic characterization and a better understanding of this frustrated system.

### 2. Experimental

**Synthesis:** Single crystals of  $\text{La}_4\text{Cu}_3\text{MoO}_{12}$  were grown by means of a molten-salt flux of  $\text{CuO}/\text{KCl}$ . A polycrystalline sample

\* Corresponding author.

E-mail address: [krp@northwestern.edu](mailto:krp@northwestern.edu) (K.R. Poeppelmeier).

<sup>1</sup> Current address: Department of Chemistry, North Carolina State University, 2620 Yarbrough Drive, Raleigh, NC 27695-8204, USA.

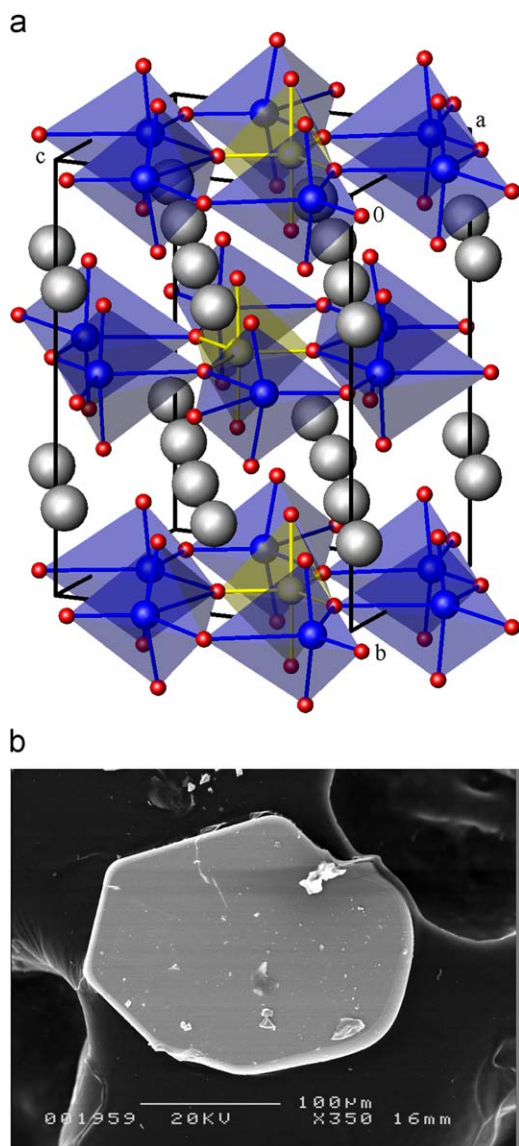


**Fig. 1.** Top: Perspective view of the fully ordered structure of  $\text{La}_4\text{Cu}_3\text{Mo}_{12}$ . Lanthanum atoms are grey and oxide ions are red. The blue and yellow bipyramidal polyhedra represent the  $\text{CuO}_5$  and  $\text{MoO}_5$  units, respectively. Bottom: Scanning electron micrograph of a  $\text{La}_4\text{Cu}_3\text{Mo}_{12}$  crystal illustrating the external hexagonal morphology that reflects the internal hexagonal symmetry of the  $\text{YAlO}_3$  sublattice. (For interpretation of the references to color in this figure legend, the reader is referred to the web version of this article.)

was prepared by annealing a stoichiometric mixture of  $\text{La}_2\text{O}_3$ ,  $\text{CuO}$  and  $\text{MoO}_3$  (all 99.99% pure) at  $1025^\circ\text{C}$  for 4 days with intermediate regrindings. For the single-crystal growth, the resulting powder was mixed with  $\text{CuO}$  and  $\text{KCl}$  in a weight ratio of 1:0.5:0.3, respectively, and placed in a platinum capsule ( $10 \times 20 \text{ mm}$ ) and sealed by folding and pressing the ends. The capsule was heated to  $1120^\circ\text{C}$  and allowed to soak for 1 h. The sample was then slowly cooled to  $900^\circ\text{C}$  at rate of  $1^\circ\text{C/h}$ , and then cooled to room temperature over 40 h. Deep red crystals of  $\text{La}_4\text{Cu}_3\text{Mo}_{12}$  were recovered from the  $\text{KCl/CuO}$  flux by washing with water and could be distinguished from the remaining  $\text{CuO}$  by their plate-like morphology. It was necessary to cut the crystals, which were often intergrown, to obtain single crystals suitable for diffraction experiments. Scanning electron microscopy (JEOL JSM-6301F) and energy dispersive X-ray spectroscopy analyses (JEOL JED-2140) were performed on multiple crystals to examine the morphology and the composition. As shown in Fig. 1 (right), the

hexagonal symmetry of the  $\text{YAlO}_3$  sublattice is reflected in the external morphology of the crystal.

**Crystallographic structure determination:** X-ray diffraction data were collected on a Bruker CCD diffractometer operating at 153 K and indicated a monoclinic unit cell with  $a=6.8560(6)\text{Å}$ ,  $b=10.9802(10)\text{Å}$ ,  $c=7.9147(7)\text{Å}$  and  $\beta=90.0160(10)^\circ$ . Relevant details regarding the data collection and refinement are given in Table 1. The structure was refined with SHELXTL [7] using the published structure (derived from powder diffraction data) as the starting model. Refinement of the structure in space group  $P2_1/m$  (no. 11), although yielding a better  $R$ -value than other space groups, initially did not produce a satisfactory solution. The observation that the  $|E^2 - 1|$  statistic used for predicting whether or not a structure is centrosymmetric was much larger (1.330) than expected for a centrosymmetric space group (0.968), and that the monoclinic  $\beta$  angle is very close to  $90^\circ$  suggested the possibility of a pseudo-merohedrally twinned structure [8]. In this situation, where the reflections from each twin component overlap, the structure emulates orthorhombic symmetry and is described by the twin law of the form  $[1\ 0\ 0/0\ -1\ 0/0\ 0\ -1]$ . The twin law describes, in matrix form, the relationship of the  $hkl$  indices of one monoclinic twin to those of the other. Introduction of twinning in the refinement reduced the  $R_1$  value from  $\sim 10\%$  to  $\sim 4\%$ . The final anisotropic structure refinement in  $P2_1/m$  converged at  $R_1=0.0396$  and  $wR_2=0.1094$ , with a data to variable ratio of over 14:1. The relative amount of each twin component was refined and converged to  $0.637(3)$ , indicating the crystal was twinned with an approximate 64:36 ratio of one twin to the other. Three other twin laws were also found to have a nearly identical effect:  $[-1\ 0\ 0/0\ -1\ 0/0\ 0\ 1]$ ,  $[-1\ 0\ 0/0\ 1\ 0/0\ 0\ 1]$ , and  $[1\ 0\ 0/0\ 1\ 0/0\ 0\ -1]$ . It should be noted that in the current study the standard setting of  $P12_1/m1$  ( $b$ =unique) was used, whereas in the previous report the authors selected the non-standard  $P112_1/m$  ( $c$ =unique) to facilitate comparisons between the various possible cation ordering patterns.

The absence of any evidence for twin domains in the electron microscopy data (*vide infra*), even though the twin law significantly improved the refinement, suggested that some disorder existed which, when averaged over the area from which diffraction information was taken, had the same effect on the diffraction pattern as a pseudo-merohedral twin law. As the major change to the structure upon application of the twin law is to change the stacking of  $\text{Cu}_3\text{MoO}_4$  layers relative to each other, the structure was refined with disordered stacking of the  $\text{Cu}_3\text{MoO}_4$  layers. Since such disordering of the stacking broke the crystal symmetry, it was necessary to refine the structure in space group  $Pm$ , the only maximal subgroup of  $P2_1/m$  whose symmetry did not constrain the relationship between the two  $\text{Cu}_3\text{MoO}_4$  layers within the unit cell. Initial refinement in space group  $Pm$  converged at  $R_1=0.0598$  and  $wR_2=0.1966$ . A partially disordered model was tested, where one of the two  $\text{Cu}_3\text{MoO}_4$  planes could be in the original position or shifted by half the unit cell in the  $c$  direction, thus allowing the ions in that layer to be disordered over two of the four possible positions while maintaining all in-plane spacings. The refinement for this partially disordered model was superior to the twin model in  $Pm$ , converging at  $R_1=0.0456$  and  $wR_2=0.1583$ . Attempts to refine a fully disordered model, with each atom disordered over all four possible positions were unsuccessful, likely due to the high number of parameters being refined simultaneously. For completeness, the same twin law as used in space group  $P2_1/m$  was also tested, but did not converge quite as well as the partially disordered model, with  $R_1=0.0503$  and  $wR_2=0.1654$ . Atomic coordinates, isotropic-equivalent displacement parameters and selected inter-atomic distances and bond angles for the partially disordered structural model in space group  $Pm$  are listed in Tables 1, 2, 3. Full structural-refinement

**Table 1**  
Single-crystal X-ray data refinement parameters for La<sub>4</sub>Cu<sub>3</sub>MoO<sub>12</sub>.

| Crystal Data                            |   | Data collection and refinement              |                           |
|---|---|---|---------------------------|
| Formula                                 | La <sub>4</sub> Cu <sub>3</sub> MoO <sub>12</sub> | Radiation ( $\lambda$ )                     | Mo K $\alpha$ (0.71073 Å) |
| Space Group                             | <i>Pm</i> (#6)                                    | Unique reflections<br>with $I > 2\sigma(I)$ | 2865<br>2465              |
| <i>a</i> (Å)                            | 6.8560(6)   | Number of parameters                        | 152                       |
| <i>b</i> (Å)                            | 10.9802(10)                                       | <i>h</i>                                    | –9 → 9                    |
| <i>c</i> (Å)                            | 7.9147(7)   | <i>k</i>                                    | –14 → 14                  |
| $\alpha$ (°)                            | 90  | <i>l</i>                                    | –10 → 10                  |
| $\beta$ (°)                             | 90.0160(10)                                       | $R[F^2 > 2\sigma(F^2)]$                     | 0.0448                    |
| $\gamma$ (°)                            | 90  | $R(F^2)$                                    | 0.0514                    |
| <i>Z</i>                                | 2   | $sR_2[F^2 > 2\sigma(F^2)]$                  | 0.1424                    |
| <i>V</i> (Å <sup>3</sup> )              | 595.82(9)   | $wR_2(F^2)$                                 | 0.1583                    |
| $d_{\text{calc}}$ (g cm <sup>–3</sup> ) | 5.765   | <i>S</i> (G.O.F.)                           | 1.107                     |
| $\mu$ (mm <sup>–1</sup> )               | 20.318  |   |                           |
| <i>T</i> (K)                            | 153(2)  |   |                           |
| Crystal shape                           | Dark red plate                                    |   |                           |
| Crystal dimensions (mm <sup>3</sup> )   | 0.034 × 0.118 × 0.116                             |   |                           |

**Table 2**  
Crystallographic data for La<sub>4</sub>Cu<sub>3</sub>MoO<sub>12</sub> based on the single crystal refinement in space group *Pm* with Mo disordered over 2 possible positions in every other layer and  $a=6.8560(6)$  Å,  $b=10.9802(10)$  Å,  $c=7.9147(7)$  Å, and  $\beta=90.0160(10)^\circ$ .

| Atom | <i>x</i>    | <i>y</i>   | <i>z</i>    | $B_{\text{eq}}$ (Å <sup>2</sup> ) <sup>a</sup> | Occupancy |
|------|-------------|------------|-------------|--|-----------|
| La1  | 0.25064(17) | 0.74998(6) | 0.11452(13) | 0.0065(4)                                      | 1         |
| La2  | 0.24841(16) | 0.75036(6) | 0.62688(13) | 0.0066(4)                                      | 1         |
| La3  | 0.76687(13) | 0.74836(6) | 0.36988(16) | 0.0067(4)                                      | 1         |
| La4  | 0.75349(15) | 0.75127(6) | 0.87158(18) | 0.0061(3)                                      | 1         |
| O1   | 0.4183(18)  | 0.8263(7)  | 0.3709(19)  | 0.0096(18)                                     | 1         |
| O2   | 0.4109(18)  | 0.8363(7)  | 0.8690(18)  | 0.0081(17)                                     | 1         |
| O3   | 0.9157(18)  | 0.8342(8)  | 0.1192(18)  | 0.009(2)                                       | 1         |
| O4   | 0.9157(19)  | 0.8328(9)  | 0.6195(19)  | 0.012(2)                                       | 1         |
| O5   | 0.0796(16)  | 0.6647(7)  | 0.8703(17)  | 0.0070(19)                                     | 1         |
| O6   | 0.5831(17)  | 0.6708(7)  | 0.6203(16)  | 0.0059(18)                                     | 1         |
| O7   | 0.5820(17)  | 0.6698(7)  | 0.1233(16)  | 0.0076(18)                                     | 1         |
| O8   | 0.0836(16)  | 0.6642(7)  | 0.3708(16)  | 0.0044(18)                                     | 1         |
| Mo1  | 0.4196(9)   | 1          | 0.3710(9)   | 0.0040(3)                                      | 1         |
| Cu1  | 0.4712(9)   | 1          | 0.8708(9)   | 0.0142(6)                                      | 1         |
| Cu2  | 0.8957(9)   | 1          | 0.0870(9)   | 0.0029(5)                                      | 1         |
| Cu3  | 0.8940(9)   | 1          | 0.6543(9)   | 0.0028(5)                                      | 1         |
| O9   | 0.763(2)    | 1          | 0.867(2)    | 0.009(3)                                       | 1         |
| O10  | 0.681(2)    | 1          | 0.3688(19)  | 0.007(3)                                       | 1         |
| O11  | 0.292(2)    | 1          | 0.5700(18)  | 0.010(3)                                       | 1         |
| O12  | 0.289(2)    | 1          | 0.1727(17)  | 0.007(2)                                       | 1         |
| Mo2A | 0.5913(17)  | 0.5        | 0.1251(16)  | 0.025(2)                                       | 0.427(12) |
| Cu4A | 0.5512(17)  | 0.5        | 0.6253(18)  | 0.000(2)                                       | 0.427(12) |
| Cu5A | 0.1069(15)  | 0.5        | 0.8440(16)  | 0.025(2)                                       | 0.427(12) |
| Cu6A | 0.1220(15)  | 0.5        | 0.3943(15)  | 0.022(2)                                       | 0.427(12) |
| O13A | 0.256(7)    | 0.5        | 0.629(6)    | 0.014(11)                                      | 0.427(12) |
| O14A | 0.303(5)    | 0.5        | 0.122(4)    | 0.000(7)                                       | 0.427(12) |
| O15A | 0.732(4)    | 0.5        | 0.921(4)    | 0.001(5)                                       | 0.427(12) |
| O16A | 0.715(5)    | 0.5        | 0.323(4)    | 0.010(6)                                       | 0.427(12) |
| Mo2B | 0.5897(14)  | 0.5        | 0.6168(13)  | 0.0148(14)                                     | 0.573(12) |
| Cu4B | 0.5480(13)  | 0.5        | 0.1211(14)  | 0.0000(14)                                     | 0.573(12) |
| Cu5B | 0.1164(12)  | 0.5        | 0.3409(13)  | 0.0204(15)                                     | 0.573(12) |
| Cu6B | 0.1110(12)  | 0.5        | 0.8983(12)  | 0.0148(14)                                     | 0.573(12) |
| O13B | 0.250(5)    | 0.5        | 0.113(4)    | 0.013(8)                                       | 0.573(12) |
| O14B | 0.306(5)    | 0.5        | 0.619(4)    | 0.006(6)                                       | 0.573(12) |
| O15B | 0.725(3)    | 0.5        | 0.419(3)    | 0.001(4)                                       | 0.573(12) |
| O16B | 0.720(3)    | 0.5        | 0.815(3)    | 0.006(5)                                       | 0.573(12) |

All disordered sites were constrained to yield a full occupancy of the site.

<sup>a</sup> Numbers listed in the  $B_{\text{eq}}$  column are the isotropic equivalent thermal displacement parameters.

details for all three structures in *Pm* and for the initial twinned refinement in *P2<sub>1</sub>/m* are given in the Supporting Information.

Bond valence sums were also calculated for all three models in space group *Pm* and for completeness are given in Supporting

**Table 3**  
Selected interatomic distances and bond angles for La<sub>4</sub>Cu<sub>3</sub>MoO<sub>12</sub>.

| Bond      | Distance (Å) | Bonds          | Angle (°) |
|-----------|--------------|----------------|-----------|
| Mo1–O10   | 1.793(13)    | O10–Mo1–O11    | 119.6(6)  |
| Mo1–O11   | 1.803(13)    | O10–Mo1–O12    | 119.2(6)  |
| Mo1–O12   | 1.807(12)    | O11–Mo1–O12    | 121.1(6)  |
| Cu1–O9    | 1.999(16)    | Cu3–O9–Cu2     | 124.2(8)  |
| Cu2–O9    | 1.966(15)    | Cu3–O9–Cu1     | 119.0(7)  |
| Cu3–O9    | 1.909(15)    | Cu2–O9–Cu1     | 116.8(7)  |
| Mo2A–O16A | 1.78(3)      | O16A–Mo2A–O15A | 120.8(14) |
| Mo2A–O15A | 1.88(3)      | O16A–Mo2A–O14A | 119.1(15) |
| Mo2A–O14A | 1.98(4)      | O15A–Mo2A–O14A | 120.1(15) |
| Cu4A–O13A | 2.03(5)      | Cu5A–O13A–Cu4A | 122(3)    |
| Cu5A–O13A | 1.99(5)      | Cu5A–O13A–Cu6A | 123(2)    |
| Cu6A–O13A | 2.07(5)      | Cu4A–O13A–Cu6A | 115(2)    |
| Mo2B–O16B | 1.81(2)      | O16B–Mo2B–O15B | 119.7(10) |
| Mo2B–O15B | 1.82(2)      | O16B–Mo2B–O14B | 119.1(13) |
| Mo2B–O14B | 1.95(3)      | O15B–Mo2B–O14B | 121.2(12) |
| Cu4B–O13B | 2.05(4)      | Cu6B–O13B–Cu5B | 123.9(18) |
| Cu5B–O13B | 2.02(4)      | Cu6B–O13B–Cu4B | 120.9(18) |
| Cu6B–O13B | 1.95(3)      | Cu5B–O13B–Cu4B | 115.2(16) |

Information [9]. In general, the bond valence sums were close to the expected values for those atoms outside of the Cu<sub>3</sub>MoO<sub>4</sub> layers. In the Cu<sub>3</sub>MoO<sub>4</sub> layers the bond valence sums were slightly closer to the expected values for the disordered model than for other models, but differences were very small. As application of bond valence sums to disordered structures is difficult and often unreliable [10], no further conclusions were based off of them.

While the partially disordered model refined the best, it was still not perfect, likely because it modeled only a portion of the disorder, and not the disorder in totality. Only the lanthanum and molybdenum atoms could be refined anisotropically: refining lighter atoms anisotropically resulted in nonpositive definite thermal parameters. For the twinned model in *Pm*, even some lanthanum and molybdenum atoms were nonpositive definite when refined anisotropically, another indication that the disordered model is a better fit. Further, there were large variations in the isotropic thermal parameters for atoms in the Cu<sub>3</sub>MoO<sub>4</sub> plane. This, however, is consistent with the fully disordered model, as those positions would be occupied by atoms of different types in the fully disordered structure. Further supporting the fully disordered model was the fact that all large residual electron density on the difference map of the partially disordered structure

was located where atoms would be located in the fully disordered structure.

**Electron microscopy:** high resolution transmission electron microscopy (HREM) and transmission electron diffraction (TED) were performed using a JEOL JEM-2100 FAST TEM and a Hitachi HF-2000 TEM, both operated at 200 kV. TED patterns were taken along the [0 1 0] and [1 0 0] zone axes using varying electron probe sizes with smallest illuminated regions around 10 nm in radius. HREM images were also taken on the [010] zone axis.

### 3. Results and discussion

**Flux growth:** A detailed understanding of a material's solid-state physics and chemistry, especially with respect to anisotropic properties, usually requires the availability of large single crystals. The flux-growth technique has been used successfully for many years to grow single crystals of complex materials such as high- $T_c$  cuprate superconductors [11]. However, the process is by no means trivial, and several factors must be considered when investigating a new system. The selection of the appropriate flux composition, growth temperature, cooling rate and starting materials, among many other factors, is critical for obtaining crystals of useful size and quality. For the current study, the choice of a CuO/KCl flux was a key to the successful growth of single crystals.

Attempts to grow  $\text{La}_4\text{Cu}_3\text{MoO}_{12}$  from a melt of the same composition (i.e., a self flux) were unsuccessful. The high temperatures required to melt the system led to significant volatilization of CuO and produced only small clear colorless crystals of  $\text{La}_2\text{MoO}_6$ . In an attempt to overcome these problems, copper oxide was chosen as a flux for two reasons: (1) to suppress the formation of  $\text{La}_2\text{MoO}_6$  and (2) to lower the melting temperature. To further minimize the vaporization of CuO, the sample was sealed in a platinum capsule. Addition of KCl allowed the facile isolation of the  $\text{La}_4\text{Cu}_3\text{MoO}_{12}$  crystals from the CuO flux and the residual starting material.

In polycrystalline samples of  $\text{La}_4\text{Cu}_3\text{MoO}_{12}$ , three distinct cation ordering patterns were observed depending on the thermal history of the sample [2]. Quenched samples showed no ordering, with the  $\text{Cu}^{2+}$  and  $\text{Mo}^{6+}$  randomly distributed over the five-coordinate metal sites. This is reflected in the unit cell and space group ( $a_h \approx 4 \text{ \AA}$ ,  $c_h \approx 11 \text{ \AA}$ ,  $P6_3/mmc$ ), which are closely related to those of  $\text{YAlO}_3$ . An intermediate cooling rate yielded partial ordering of the cations and consequently a larger unit cell ( $a_o \approx a_h \approx 4 \text{ \AA}$ ,  $b_o \approx \sqrt{3}a_h \approx 6.9 \text{ \AA}$ ,  $c_o \approx c_h \approx 11 \text{ \AA}$ ,  $Pmnm$ ). Finally, slower cooling at a rate of  $36^\circ/\text{h}$  allowed the cations to order fully within each  $\text{Cu}_3\text{MoO}_4$  layer and gave the monoclinic unit cell ( $a_m \approx 2a_h \approx 8 \text{ \AA}$ ,  $b_m \approx \sqrt{3}a_h \approx 6.9 \text{ \AA}$ ,  $c_m \approx c_h \approx 11 \text{ \AA}$ ,  $\gamma \approx 90^\circ$ ,  $P112_1/m$ ) with a triangular arrangement of coppers. The existence of these three possible phases dictated the use of the slow cooling rate.

**Structural disorder and electron microscopy:** The lattice parameters determined from the single crystal data agree very well (all within 0.3%) with those reported previously based on polycrystalline samples for the fully ordered structure. The three  $\text{Cu}^{2+}$  cations and the single  $\text{Mo}^{6+}$  cation occupy four distinct five-coordinate ( $\text{MO}_{3/3+2}$ ) sites that share vertices to form  $\text{Cu}_3\text{MoO}_4$  layers separated by O/La/O layers, as shown in Fig. 1 (top). The  $\text{Cu}_3\text{MoO}_4$  planes can be envisioned as isolated  $\text{Cu}_3\text{O}$  triangles separated by  $\text{MoO}_3$  units, as illustrated for a single layer in Fig. 2. The three coppers that make up the triangles are significantly shifted towards the central oxygen, O(9), as reflected by the average in-plane Cu–O bond length, which is 1.988 Å in the triangles while it is 2.687 Å outside of them. These compare well to the values determined previously of 1.983 and 2.690 Å,

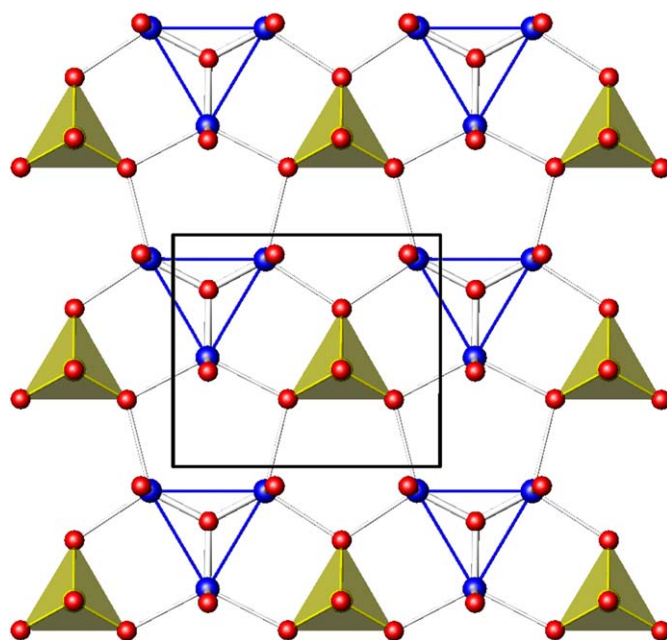


**Fig. 2.** Structural view of a single layer of the triangular lattice of  $\text{La}_4\text{Cu}_3\text{MoO}_{12}$  perpendicular to the  $b$ -axis. The copper atoms are blue, the oxide ions are red and the  $\text{MoO}_5$  trigonal bipyramids are yellow. The isolated triangular clusters of  $\text{Cu}_3\text{O}$  are outlined by the thin blue lines. The relatively short intra-triangle bonds are thick, while the longer inter-triangle bonds are thin. The thick black line denotes the  $ac$ -face of the unit cell. (For interpretation of the references to color in this figure legend, the reader is referred to the web version of this article.)

respectively. From the present structural determination it seems the triangles are slightly more regular than previously reported: the Cu–O–Cu angles for the layer without disorder are  $116.8(7)^\circ$ ,  $119.0(7)^\circ$ , and  $124.2(8)^\circ$  as opposed to  $121.1^\circ$ ,  $115.3^\circ$  and  $123.6^\circ$ . Unlike previous refinements, the apical bond lengths are completely isometric due to the mirror plane; although the average lengths are similar, 1.850 Å versus 1.841 Å. The smaller  $\text{MoO}_5$  unit has an average Mo–O bond length of 1.836 Å in-plane and 1.889 Å apical, and is also more regular than previously reported, with in-plane angles ranging from  $119.1^\circ$  to  $121.2^\circ$  versus  $116.0^\circ$  to  $124.0^\circ$ . Although unusually low for such a large cation, the coordination of the lanthanum cations is 6+2 and the bond lengths are comparable to those reported by Vander Griend et al [2]. While powder diffraction techniques were able to yield many features of the structure and show many similarities to the results from single crystal diffraction and TEM, there were several key structural elements that the powder diffraction was unable to determine.

Although the single-crystal growth experiments yielded a structure fully ordered in two dimensions, it was necessary to investigate whether disorder was present in the stacking of the  $\text{Cu}_3\text{MoO}_4$  planes or if the twinned structural model was correct. The TED pattern along the [0 1 0] zone axis is shown in Fig. 3, with the horizontal axis along (0 0 1) (in reciprocal space) and the vertical axis along (100) direction. In a single twin domain, there should be a noticeable difference in intensity between the (1 0 1)/ $(-1 0 -1)$  spot pair and the  $(-1 0 1)/(1 0 -1)$  spot pair, and which pair is more intense should be inverted at each twin boundary. While this might disappear due to dynamical effects if diffraction is taken from a large volume, they should be noticeable in local diffraction from small volumes and thin regions, where dynamical diffraction are much less of an issue. The absence of any such differences indicates that either there are no twin domains, or they are so small that even the very small electron

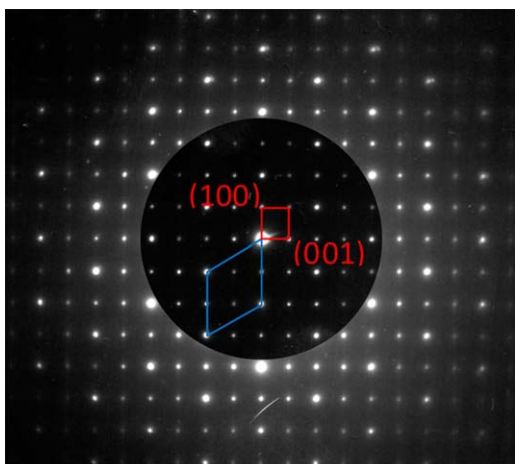


**Fig. 3.** Electron diffraction pattern along the  $[0\ 1\ 0]$  zone axis. Monoclinic unit cell in red, pseudo-hexagonal sub-cell in blue. (For interpretation of the references to color in this figure legend, the reader is referred to the web version of this article.)

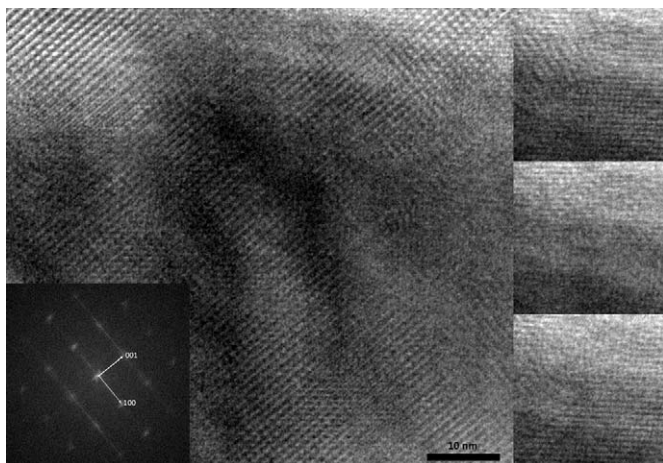


**Fig. 4.** Left: HREM image taken on the  $[0\ 1\ 0]$  zone axis with Fourier transform insert. Right: post-processed images of a smaller region taken at three different foci (32 nm focus step). The processing involved performing a Fourier transform, masking spots besides the  $(1\ 0\ 1)$ ,  $(-1\ 0\ 1)$ ,  $(-1\ 0\ -1)$ , and  $(1\ 0\ -1)$  spots of interest, and performing an inverse Fourier transform. This leaves an image dominated by the  $(1\ 0\ 1)$  and  $(-1\ 0\ 1)$  lattice fringes.

probes ( $\sim 10$  nm radius) diffracted from multiple domains simultaneously. In addition, HREM images were taken along the  $[001]$  zone axis, shown in Fig. 4, and processed by applying a Fourier transform, masking the spots besides the  $(1\ 0\ 1)$ ,  $(-1\ 0\ 1)$ ,  $(-1\ 0\ -1)$ , and  $(1\ 0\ -1)$  reflections of interest, and applying an inverse Fourier transform. This procedure leaves an image dominated by the  $(1\ 0\ 1)$  and  $(-1\ 0\ 1)$  lattice fringes. Each twin domain would be dominated by one or the other set of lattice fringes, with twin boundaries visible by the change in which set of lattice fringes dominates. However, such differences are minimal and also change with focus, thus indicating that twin domains are present. The electron diffraction pattern along the  $[1\ 0\ 0]$  zone axis is shown in Fig. 5, with shorter exposure times overlaid over the center of longer exposure times. The diffuse scattering, primarily manifested as lines along  $(0\ 0\ 1)$ , indicates real space frustration in the ordering in the perpendicular  $[0\ 1\ 0]$  direction.

While a pseudo-merohedral twin law was originally used in the structural refinement to account for this disorder, the HREM

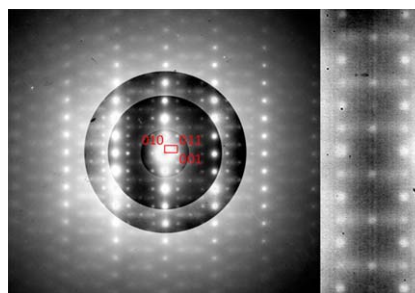


**Fig. 5.** Left: Electron diffraction pattern along the  $[1\ 0\ 0]$  zone axis with shorter exposure times overlaid over center of longer exposure times. Right: Close up of diffuse lines, marked with arrows. Unit cell in red. (For interpretation of the references to color in this figure legend, the reader is referred to the web version of this article.)

and TED data revealed that no twin boundaries or twin domains could be found. The initially proposed twin law, i.e.,  $[1\ 0\ 0/0\ -1\ 0/0\ 0\ -1]$ , is equivalent to a  $180^\circ$  rotation around the  $a$ -axis, and the other three are equivalent to a  $180^\circ$  rotation around the  $c$ -axis, a mirror on the  $bc$ -plane, and a mirror on the  $ab$ -plane. Any of these operations, when applied to the structure in real space and combined with an appropriate translation yields a structure that keeps the hexagonal sub-cell unchanged. Any such twinning would leave the lanthanum layer virtually unchanged, and would leave all in-plane relationships unchanged for the  $\text{Cu}_3\text{MoO}_4$  layers. The only significant change brought about would be in the stacking of one  $\text{Cu}_3\text{MoO}_4$  layer relative to the next: in different  $\text{Cu}_3\text{MoO}_4$  layers the  $\text{Cu}^{2+}$  cations could occupy different positions. A structural view down the  $a$ -axis of  $\text{La}_4\text{Cu}_3\text{MoO}_{12}$  is shown in Fig. 6, with the proposed twin boundary given by the green line. The two different twin domains match up nearly perfectly, the only difference being which  $\text{MO}_5$  polyhedra contain the Mo atom and which contain the Cu atoms. This is equivalent to disorder in the stacking between the layers, but preserving perfect intra-layer ordering. However, no distinct twin domains could be found, and thus the structure is more accurately described as disordered.

While twin domains were not in fact observed, at least not with a twin domain size greater than the distance between  $\text{Cu}_3\text{MoO}_4$  layers, the twin law successfully modeled a disorder in the stacking of the  $\text{Cu}_3\text{MoO}_4$  layers. As changing the order of the  $\text{Cu}_3\text{MoO}_4$  layer stacking broke symmetry, it was necessary to refine the structure in space group  $Pm$  to confirm the disorder model. In space group  $P2_1/m$  and in all other maximal subgroups thereof, the positions of the atoms in the second  $\text{Cu}_3\text{MoO}_4$  layer were dependent on the positions of those in the first  $\text{Cu}_3\text{MoO}_4$  layer. In space group  $Pm$ , however, the  $\text{Cu}_3\text{MoO}_4$  layer lies in the mirror plane, and thus all atoms in both  $\text{Cu}_3\text{MoO}_4$  layers are independent. A significant improvement in refinement was found when removing the dependence of one  $\text{Cu}_3\text{MoO}_4$  layer on another even before disorder was introduced, indicating that the  $\text{Cu}_3\text{MoO}_4$  layers are independent. This was confirmed by the further improvement in refinement when the disorder was introduced to the model. The inclusion of disorder in  $\text{Cu}_3\text{MoO}_4$  layer stacking had a very similar effect to the inclusion of a twin law, i.e., the atomic positions in the model with disorder and the model with the pseudo-merohedral twin were very similar. The disordered structural model is further supported by the observation of diffuse scattering in TED patterns taken along the  $[100]$  zone axis. Including more than two different stacking possibilities in the disorder model resulted in too many independent variables, and an unstable refinement. While the partially disordered model is a very good approximation, we believe that the actual structure is fully disordered with respect to the stacking of the  $\text{Cu}_3\text{MoO}_4$  layers.

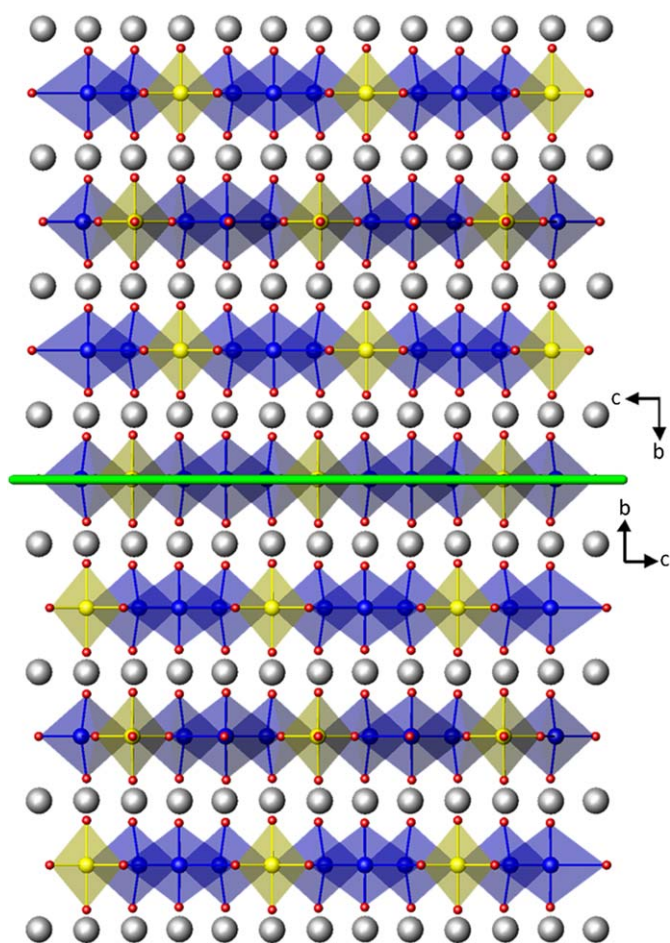


**Fig. 6.** View down the  $a$ -axis of  $\text{La}_4\text{Cu}_3\text{MoO}_{12}$  with the proposed twin boundary, shown by the green line. The twinning model is equivalent to disorder in the stacking between the layers, but preserving perfect intra-layer ordering. Copper atoms occupy blue polyhedra, molybdenum atoms occupy yellow polyhedra, and the lanthanum atoms are gray. (For interpretation of the references to color in this figure legend, the reader is referred to the web version of this article.)

#### 4. Conclusions

The ability to grow sizable single crystals of the complex cuprate  $\text{La}_4\text{Cu}_3\text{MoO}_{12}$  makes possible detailed (anisotropic) electron spin resonance, magnetic and electronic studies of this interesting material. Furthermore, the synthetic strategies laid out herein may be beneficial for the crystal growth of other copper-containing complex oxides. For example, the related compound  $\text{La}_3\text{Cu}_2\text{VO}_9$  displays a stunningly complicated ordering scheme [12,13] which would benefit from single crystal diffraction data to confirm the structure as determined from polycrystalline powders. Finally, while modern powder diffraction techniques were

able to yield a great deal of structural information, more sophisticated techniques are required to solve complex problems, such as the structure of  $\text{La}_4\text{Cu}_3\text{MoO}_{12}$ .

**Supporting Information:** The crystallographic information files can be obtained from the Fachinformationzentrum Karlsruhe, 76344 Eggenstein-Leopoldshafen, Germany (e-mail: [crysdata@fiz.karlsruhe.de](mailto:crysdata@fiz.karlsruhe.de)) on quoting the Registry nos. CSD-421355 (disordered refinement in  $Pm$ ) and CSD-421356 (twinned refinement in  $Pm$ ).

#### Acknowledgments

The authors would like to thank Chris S. Own, Julien Lesage, Job T. Rijssenbeek, and Charlotte L. Stern for their contributions to this work. The authors acknowledge the support from the *National Science Foundation* (Solid State Chemistry Award No. DMR-0604454); the use of TEMs in the EPIC facility of the NUANCE Center of Northwestern University supported by NSP-NSEC, NSF-MRSEC, Keck Foundation, the State of Illinois, and Northwestern University; and the use of the Central Facilities supported by the MRSEC program of the *National Science Foundation* (DMR-0520513) at the Materials Research Center of Northwestern University.

#### Appendix A. Supplementary material

Supplementary data associated with this article can be found in the online version at [doi:10.1016/j.jssc.2009.11.019](https://doi.org/10.1016/j.jssc.2009.11.019).

#### References

- [1] A.P. Ramirez, *Annu. Rev. Mater. Sci.* 24 (1994) 453–480.
- [2] D.A. Vander Griend, S. Boudin, V. Caignaert, K.R. Poeppelmeier, Y.G. Wang, V.P. Dravid, M. Azuma, M. Takano, Z.B. Hu, J.D. Jorgensen, *J. Am. Chem. Soc.* 121 (1999) 4787–4792.
- [3] M. Azuma, T. Odaka, M. Takano, D.A. Vander Griend, K.R. Poeppelmeier, Y. Narumi, K. Kindo, Y. Mizuno, S. Maekawa, *Phys. Rev. B* 62 (2000) R3588–R3591.
- [4] S. Wessel, S. Haas, *Phys. Rev. B* 63 (2001) 140403.
- [5] H.T. Wang, *Phys. Rev. B* 64 (2001) 174410.
- [6] Y. Qiu, C. Broholm, S. Ishiwata, M. Azuma, M. Takano, R. Bewley, W.J.L. Buyers, *Phys. Rev. B* 71 (2005) 214439.
- [7] SHELXTL; Bruker-AXS, Inc., Madison, WI, 1997.
- [8] G.M. Sheldrick, In *SHELXTL Reference Manual*, Bruker-AXS Inc., Madison, WI, 1997.
- [9] I.D. Brown, D. Altermatt, *Acta Crystallogr. Sect. B Struct. Sci.* 41 (1985) 244–247.
- [10] K.R. Heier, K.R. Poeppelmeier, *J. Solid State Chem.* 133 (1997) 576–579.
- [11] C. Changkang, *Prog. Crystal Growth and Charact.* 24 (1992) 213–267.
- [12] S. Malo, D.A. Vander Griend, K.R. Poeppelmeier, Y.G. Wang, V.P. Dravid, *Solid State Sci.* 3 (2001) 17–23.
- [13] D.A. Vander Griend, S. Malo, S.J. Barry, N.M. Dabbousch, K.R. Poeppelmeier, V.P. Dravid, *Solid State Sci.* 3 (2001) 569–579.